

## Energy Model of Bilayer Nanoplate Scrolling: Formation of Chrysotile Nanoscroll

A. A. Krasilin and V. V. Gusarov

*St. Petersburg State Institute of Technology, Moskovskii pr. 26, St. Petersburg, 194013 Russia*  
*e-mail: ikrasilin@gmail.com*

Received May 14, 2015

**Abstract**—Energy model of formation of multiwall nanoscrolls from thin layers has been proposed. The three major factors favoring the scrolling are dimensional mismatch of the crystal lattices forming the bilayer, difference of the surface energy at the bilayer sides, and the interaction between the bilayers. Optimal cross-section geometry of the finite-length nanoscrolls with chrysotile structure has been simulated. Effects of the Young's modulus, specific surface energy, and adhesion energy on the nanoscroll morphology have been considered.

**Keywords:** inorganic nanotubes, multiwall nanotube, simulation

**DOI:** 10.1134/S1070363215100047

The ability to spontaneously form tubular particles has been recognized as a characteristic feature of many layered substances including quasi-2D crystal lattices of molybdenum and tungsten disulfides [1], vanadium oxide [2–4], hydrosilicates of chrysotile, halloysite, and imogolite types [5–15], etc [16–19]. The basic condition for formation of nanoscrolls based on such compounds is the absence of the symmetry plane in the precursor layer. The difference in the surface energy of the opposite sides of the layer and (in the case of the bilayer) the dimensional mismatch of the constituting polyhedral lattices act as the driving forces of the layer scrolling. These forces can be either co-directed or competitive. Generally speaking, the similar reasons result in the scrolling of, non-monocrystalline artificial layers described, for instance, in [20–22]. Understanding of the features of formation and growth of the nanotubes and nanoscrolls is crucial for preparation of nanotubular structures.

Formation of a single-wall nanotube and a nanoscroll during bending of a thin bilayer plate (the nanotubulene being considered infinitely long) has been examined in [23] using the chrysotile-type magnesium hydrosilicate as an example. In practice, majority of the above-listed compounds form multi-wall nanoscrolls of finite length [24]. In view of this, the present work extended the proposed model for the

case of the formation of finite-length multiwall nanoscroll and analyzed the influence of energy, mechanical, and structural parameters on the product morphology.

The assumptions made during the model derivation have been discussed in detail elsewhere [23]. Even though the layer scrolling could be accompanied by physical and chemical changes [25], hereafter we will only consider the process changing the morphology. Similarly to [23], the Young's modulus, the specific surface energy, and the adhesion energy will be considered independent of the layer thickness and curvature. In the case of the multiwall tube the energy is calculated via summation over each of the bilayers; this seriously complicates the calculations in the case of a large number of the bilayers. Therefore, in this work we will exclusively consider the scroll geometry with the energy being determined via integration over the spiral length.

In the case of the nanoscroll folding following the scheme in Fig. 1, the change of the total energy could be expressed as sum of three major components with respect to the amount of matter  $v$  [Eq. (1)]:

$$\Delta E = \frac{1}{v} (\Delta E_d + \Delta E_s - U_a), \quad (1)$$

with  $\Delta E_d$ , change of the elastic energy;  $\Delta E_s$ , change of the surface energy; and  $U_a$ , energy of the interlayer

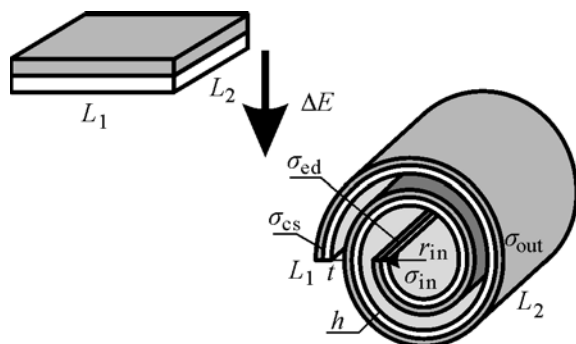


**Fig. 1.** Scheme of the finite-size bilayered nanoscroll formation.

interaction appearing when the bilayer is scrolls for more than one turn.

The change of the elastic energy is determined as the difference of the elastic energies of the scroll and the plane. The equations derived in [23] should have been modified to account for the finite size of the bilayer; that gave Eq. (2) for the elastic energy of the scroll.

$$E_d^@ = \frac{D}{2} L_2 \int_0^{2\pi n} \Delta c^2(\varphi) F(\varphi) d\varphi. \quad (2)$$

Here  $D = Yh^3/[12(1 - \mu^2)]$ , bending stiffness;  $Y$ , the Young's modulus;  $h$ , the bilayer thickness;  $\mu$ , the Poisson's ratio;  $L_2$ , the nanoscroll length;  $n$ , the number of layers;  $\Delta c^2(\varphi) = [1/(r_{in} + f\varphi) - 1/r_0]^2$ ;  $r_{in}$ , inner radius of the nanoscroll;  $f = (h + t)/2\pi$ , the Archimedean spiral constant;  $r_0$ , radius of the mechanically unstressed bilayer;  $\varphi$ , the polar coordinate;  $F(\varphi) = \sqrt{f^2 + (r_{in} + f\varphi)^2}$ , length of the integration element.

Elastic energy of the finite-size bilayer can be determined using Eq. (3), the  $L_1$  being the length in the direction of scrolling.

$$E_d^- = \frac{D}{2r_0^2} L_1 L_2, \quad (3)$$

Surface energy of the planar bilayer was calculated in the rectangles approximation for each of the six surfaces (Fig. 1). In the case of a scroll, the surface area is calculated via integration over the length of the corresponding spiral. Energy of the interlayer interaction favors reducing of the surface energy; the former is calculated via integration over the spiral length as

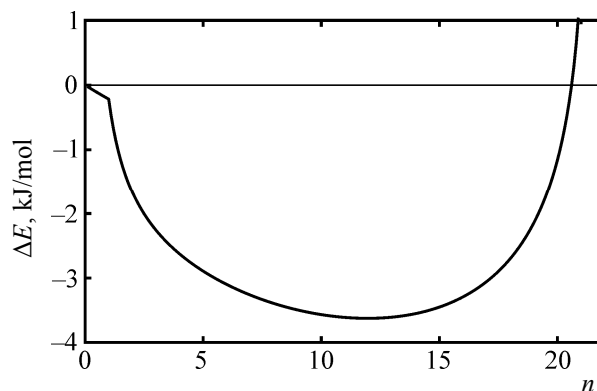


**Fig. 2.** Change of energy as function of the number of layers of the nanoscroll.

well, the integration limits corresponding to the area between the bilayers.

The energy gain due to scrolling of the chrysotile-type layer was calculated using the following limits and values of the parameters: the Young's modulus of 100 to 1000 GPa with characteristic value  $Y$  of 300 GPa [26–28], the Poisson's ratio  $\mu$  of 0.2, radius of the mechanically relaxed bilayer  $r_0$  of 8.8 nm [29], the bilayer thickness  $h$  of 0.4 nm, and the interlayer spacing  $t$  of 0.3 nm [24]. Specific surface energy of the interlayer interaction was varied from 0.001 to 0.1 J/m<sup>2</sup>. Specific surface energy of the brucite-type lattice of the [MgO<sub>6</sub>] octahedrons was varied from 0.001 to 2 J/m<sup>2</sup>. Specific surface energy of the pseudo hexagonal lattice of the [SiO<sub>4</sub>] tetrahedrons and the scroll faces was taken equal to 0.3 and 0.45 J/m<sup>2</sup>, respectively.

Figure 2 displays the change of total energy  $\Delta E(n)$  after scrolling of a square plate of  $1 \times 1 \mu\text{m}^2$ . At the initial bending stage ( $n < 1$ ), slight energy gain was observed due to relaxation of the inner stress. Scrolling by more than one turn results in steep decrease of the energy associated with the interaction between the bilayers. The  $\Delta E(n)$  dependence revealed the energy minimum with certain parameters: the inner radius and the number of layers. Further scrolling was energetically unfavorable.

In order to elucidate the effect of the scroll energy terms on the cross-section geometry, we varied the following model parameters: the Young's modulus, specific surface energy of the outer layer, and specific energy of the interlayer interaction. The choice of the parameters was based on the experimentally observed

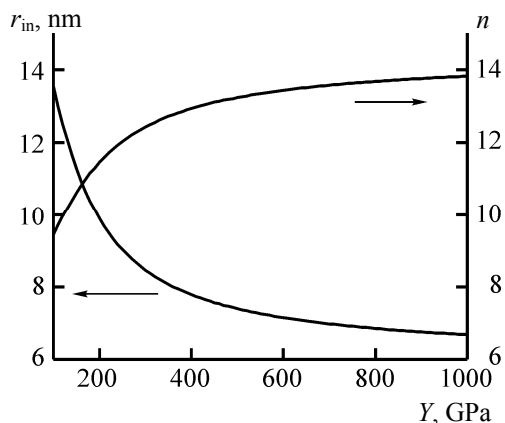


**Fig. 3.** Geometry parameters of the nanoscroll cross-section corresponding to the energy minimum, as function of the Young's modulus.

variations of the Young's modulus [27, 28] and the changes of the surface energy or the interlayer interaction energy due to sorption of different species or deprotonation.

Increase of the Young's modulus (Fig. 3) resulted in the decrease of the inner radius approaching a certain constant limit, whereas the number of layers was increased. That allowed folding of the layer to arrange the maximum number of turns close to  $r_0$ . Increase of specific surface energy at the side of the  $[\text{MgO}_6]$  octahedrons lattice led to unscrolling (increase of the inner radius and decrease of the number of layers) (Fig. 4). Increase of the adhesion energy favored additional scrolling to maximize the area of the scroll located in the interlayer space.

The model described in this work revealed the influence of structural and chemical factors as well as the synthesis conditions of formation of finite-length multiwall nanoscrolls including those of chrysotile type. The scrolling phenomenon could be represented as a consequence of three competing factors: the elastic energy tending to stabilize the nanoscroll at the curvature radius close to  $r_0$  with the lowest inner stress, the surface energy tending to reduce the surface area with the high excess energy, and the adhesion energy tending to increase the surface area accommodated inside the interlayer space. The presence of the scroll length  $L_2$  in the equations will allow further analysis of that competition influence on the scroll shape, of the recrystallization features, and of the patterns of the axial and radial growth. The derived energy-related approach is applicable for analysis of formation of nanoscrolls from thin layers.

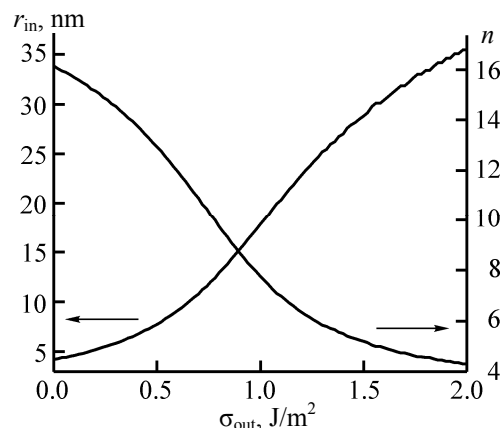


**Fig. 4.** Geometry parameters of the nanoscroll cross-section corresponding to the energy minimum, as function of specific surface energy of the outer surface.

## ACKNOWLEDGMENTS

This work was financially supported by the Ministry of Education and Science of Russian Federation in the frame of the governmental contract no. 876.

## REFERENCES

1. Tenne, R., Margulis, L., Genut, M., and Hodes, G., *Nature*, 1992, vol. 360, no. 6403, p. 444. DOI: 10.1038/360444a0.
2. Volkov, V.L., Zakharova, G.S., and Kuznetsov, M.V., *Russ. J. Inorg. Chem.*, 2004, vol. 49, no. 7, p. 1068.
3. Grigor'eva, A.V., Anikina, A.V., Tarasov, A.B., Gudilin, E.A., Knot'ko, A.V., Volkov, V.V., Dembo, K.A., and Tret'yakov, Yu.D., *Doklady Chem.*, 2006, vol. 410, no. 2, p. 165. DOI: 10.1134/S0012500806100016.
4. Semenenko, D.A., Itkis, D.M., Kulova, T.L., Yashuk, T.S., Skundin, A.M., Goodilin, E.A., and Tret'yakov, Y.D., *Electrochim. Acta*, 2012, vol. 63, p. 329. DOI: 10.1016/j.electacta.2011.12.116.
5. Bates, T.F., Sand, L.B., and Mink, J.F., *Science*, 1950, vol. 111, no. 2889, p. 512.
6. Korytkova, E.N., Maslov, A.V., Pivovarova, L.N., Drozdova, I.A., and Gusarov, V.V., *Glass Physics Chem.*, 2004, vol. 30, no. 1, p. 51. DOI: 10.1023/B:GPAC.0000016397.29132.21.
7. Falini, G., Foresti, E., Gazzano, M., Gualtieri, A.F., Leoni, M., Lesci, I.G., and Roveri, N., *Chemistry*, 2004, vol. 10, no. 12, p. 3043. DOI: 10.1002/chem.200305685.
8. Jancar, B. and Suvorov, D., *Nanotechnology*, 2006, vol. 17, no. 1, p. 25. DOI: 10.1088/0957-4484/17/1/005.
9. Krasilin, A.A., Almjasheva, O.V., and Gusarov, V.V.,

- Inorg. Mater.*, 2011, vol. 47, no. 11, p. 1111. DOI: 10.1134/S002016851110013X.
10. Bates, T.F., Hidebrand, F.A., and Swineford, A., *Am. Mineral.*, 1950, vol. 35, nos. 7–8, p. 463.
  11. Singh, B. and Mackinnon, I.D.R., *Clays Clay Miner.*, 1996, vol. 44, no. 6, p. 825.
  12. White, R.D., Bavykin, D.V., and Walsh, F.C., *J. Phys. Chem. (C)*, 2012, vol. 116, no. 15, p. 8824. DOI: 10.1021/jp300068t.
  13. White, R.D., Bavykin, D.V., and Walsh, F.C., *Nanotechnology*, 2012, vol. 23, no. 6, p. 065705. DOI: 10.1088/0957-4484/23/6/065705.
  14. Yang, H., Wang, C., and Su, Z., *Chem. Mater.*, 2008, vol. 20, no. 13, p. 4484. DOI: 10.1021/cm8001546.
  15. Levard, C., Rose, J., Thill, A., Masion, A., Doelsch, E., Maillet, P., Spalla, O., Olivi, L., Cognigni, A., Ziarelli, F., and Bottero, J.-Y., *Chem. Mater.*, 2010, vol. 22, no. 8, p. 2466. DOI: 10.1021/cm902883p.
  16. Tenne, R. and Rao, C.N.R., *Philos. Trans. (A)*, 2004, vol. 362, no. 1823, p. 2099. DOI: 10.1098/rsta.2004.1431.
  17. Tenne, R., *Nat. Nanotechnol.*, 2006, vol. 1, no. 2, p. 103. DOI: 10.1038/nnano.2006.62.
  18. Rao, C.N.R. and Govindaraj, A., *Adv. Mater.*, 2009, vol. 21, no. 42, p. 4208. DOI: 10.1002/adma.200803720.
  19. Radovsky, G., Popovitz-Biro, R., and Tenne, R., *Chem. Mater.*, 2014, vol. 26, no. 12, p. 3757. DOI: 10.1021/cm501316g.
  20. Prinz, V.Y., *Microelectron. Eng.*, 2003, vol. 69, nos. 2–4, p. 466. DOI: 10.1016/S0167-9317(03)00336-8.
  21. Gulina, L.B. and Tolstoy, V.P., *Russ. J. Gen. Chem.*, 2014, vol. 84, no. 8, p. 1472. DOI: 10.1134/S1070363214080039.
  22. Tolstoy, V.P. and Gulina, L.B., *Langmuir*, 2014, vol. 30, no. 28, p. 8366. DOI: 10.1021/la501204k.
  23. Krasilin, A.A. and Gusarov, V.V., *Russ. J. Gen. Chem.*, 2014, vol. 84, no. 12, p. 2359. DOI: 10.1134/S1070363214120019.
  24. Roveri, N., Falini, G., Foresti, E., Fracasso, G., Lesci, I.G., and Sabatino, P., *J. Mater. Res.*, 2006, vol. 21, no. 11, p. 2711. DOI: 10.1557/jmr.2006.0359.
  25. Rusanov, A.I., *Surf. Sci. Rep.*, 2014, vol. 69, no. 4, p. 296. DOI: 10.1016/j.surfrep.2014.08.003.
  26. Lourenço, M.P., de Oliveira, C., Oliveira, A.F., Guimarães, L., and Duarte, H.A., *J. Phys. Chem. C*, 2012, vol. 116, no. 17, p. 9405. DOI: 10.1021/jp301048p.
  27. Piperno, S., Kaplan-Ashiri, I., Cohen, S.R., Popovitz-Biro, R., Wagner, H.D., Tenne, R., Foresti, E., Lesci, I.G., and Roveri, N., *Adv. Funct. Mater.*, 2007, vol. 17, no. 16, p. 3332. DOI: 10.1002/adfm.200700278.
  28. Nyapshaev, I.A., Shcherbin, B.O., Ankudinov, A.V., Kumzerov, Yu.A., Nevedomskii, V.N., Krasilin, A.A., Al'myasheva, O.V., and Gusarov, V.V., *Nanosistemy: Fiz., Kim., Matem.*, 2011, vol. 2, no. 2, p. 48.
  29. Cressey, B.A. and Whittaker, E.J.W., *Mineral. Mag.*, 1993, vol. 57, no. 389, p. 729. DOI: 10.1180/minmag.1993.057.389.17.